The International Journal of Cardiovascular Imaging (2019) 35:587–595
https://doi.org/10.1007/s10554-018-1506-y

ORIGINAL PAPER

Automatic coronary blood flow computation: validation in quantitative flow ratio from coronary angiography

Yimin Zhang[1,2] · Su Zhang[1,2] · Jelmer Westra[3] · Daixin Ding[1,2] · Qiuyang Zhao[1,2] · Junqing Yang[4] · Zhongwei Sun[5] · Jiayue Huang[1,2] · Jun Pu[6] · Bo Xu[5] · Shengxian Tu[1,2,6]

Received: 5 September 2018 / Accepted: 16 November 2018 / Published online: 8 December 2018

Abstract

To assess a novel approach for automatic flow velocity computation in deriving quantitative flow ratio (QFR) from coronary angiography. QFR is a novel approach for assessment of functional significance of coronary artery stenosis without using pressure wire and induced hyperemia. Patient-specific coronary flow is estimated semi-automatically by frame count method, which is subjective and inconvenient in the workflow of QFR analysis. The vascular structures were automatically delineated from coronary angiogram. Subsequently, the centerline of the interrogated vessel was extracted from the delineated lumen on each image frame and the change in the length of centerline was used to compute the flow velocity, which provided patient-specific flow for computation of QFR (QFR_{auto}). A parameter derived from the increase in centerline length was used to automatically quantify the stability of contrast flow. From the two angiographic image runs used for three-dimensional angiographic reconstruction, the one with better stability was used to compute QFR_{auto}. QFR_{auto} was assessed in all patients enrolled in the FAVOR II China study, and compared with the commercialized QFR computational method based on frame count (QFR_{count}), using pressure wire-based fractional flow reserve (FFR) as the reference standard. Out of 328 vessels with paired FFR data, QFR_{auto} was successfully computed on 325 (99%) vessels with acceptable stability in filling of contrast flow. The flow velocity computed by the proposed approach had a weak to moderate correlation with the frame count method ($r=0.37$, $p<0.001$), with mean differences of -0.02 ± 0.07 m/s ($p<0.001$). QFR_{auto} had good correlation ($r=0.96$, $p<0.001$) and agreement (mean difference: -0.01 ± 0.04, $p<0.001$) with QFR_{count}. Good correlation ($r=0.83$, $p<0.001$) and agreement (mean difference: 0.01 ± 0.06, $p=0.016$) were also observed between QFR_{auto} and FFR. Using $FFR\leq0.80$ to define functional significance of coronary stenosis, the overall diagnostic accuracy for QFR_{auto} was 93.2% (95% CI 90.5–96.0%). The area under the receiver-operating characteristic curve did not differ significantly between QFR_{count} and QFR_{auto} (difference: 0.00; 95% CI −0.01 to 0.01; $p=0.529$). Sensitivity, specificity, positive likelihood ratio, and negative likelihood ratio for QFR_{auto} were 92.4% (95% CI 86.0–96.5%), 93.7% (95% CI 89.5–96.6%), 14.7 (95% CI 8.7–25.0), and 0.1 (95% CI 0.0–0.2), respectively. Automatic computation of patient-specific coronary flow velocity based on coronary angiography is feasible. Assessment of QFR based on this novel approach had good diagnostic accuracy in determining the functional significance of coronary stenosis.

Keywords Fractional flow reserve · Quantitative flow ratio · Coronary blood flow · Coronary angiography · Image processing

✉ Shengxian Tu
sxtu@sjtu.edu.cn

[1] Biomedical Instrument Institute, School of Biomedical Engineering, Shanghai Jiao Tong University, Shanghai, China

[2] Shanghai Med-X Engineering Research Center, Shanghai Jiao Tong University, Shanghai, China

[3] Department of Cardiology, Aarhus University Hospital, Skejby, Denmark

[4] Guangdong General Hospital, Guangzhou, China

[5] Fu Wai Hospital, National Center for Cardiovascular Diseases, Chinese Academy of Medical Sciences, Beijing, China

[6] Renji Hospital, Shanghai Jiao Tong University School of Medicine, Shanghai, China

Abbreviations

AUC	Areas under the receiver-operator characteristics curve
CI	Confidence interval
FFR	Fractional flow reserve
LAD	Left anterior descending
QFR	Quantitative flow velocity
QFR_{auto}	QFR computed by V_{auto}
QFR_{count}	QFR computed by V_{count}
RCA	Right coronary artery
V_{auto}	Automatically calculated flow velocity
V_{count}	Frame count-based flow velocity

Introduction

Fractional flow reserve (FFR) is a precise index for assessment of physiological significance of coronary stenosis. Favorable outcomes for FFR-guided coronary intervention have been documented by numerous clinical studies [1–5]. Nevertheless, the clinical adoption of FFR is still poor in general because of the cost of pressure wires and the limitations associated with the use of vasodilators to induce maximum hyperemia.

Quantitative flow ratio (QFR) is a novel approach for rapid estimation of FFR pullbacks without using pressure wires or inducing hyperemia [6, 7]. QFR analysis is based on the three-dimentional reconstruction and fluid dynamics algorithms [8–10]. Calculation of patient-specific blood flow velocity is prerequisite for the computation of QFR. Current commercialized QFR applications use semi-automatic frame count method to calculate flow velocity, which is subject to inter and intra-observer variability and inconvenient in the workflow of QFR analysis.

The aim of this study was to propose a novel approach for automatic flow velocity computation to derive QFR from coronary angiography (QFR_{auto}). QFR_{auto} was compared with QFR computed using semi-automatic frame count (QFR_{count}), using pressure wire-based FFR as the reference standard.

Methods

Study design and materials

This study reports an ad hoc analysis of the FAVOR II China study, a prospective and multicenter study enrolling patients who had at least one lesion with a 30–90% diameter stenosis by visual estimation, designed to validate the diagnostic accuracy of QFR. The study design and the primary results were presented in the main publication [8]. The QFR analysis procedure includes three-dimensional (3D) geometry reconstruction, evaluation of patient-specific coronary flow, and pressure drop and QFR computation using a novel algorithm [6]. In the main publication [8], patient-specific coronary flow was evaluated using frame count method (V_{count}). The present study used a new method to automatically calculate patient-specific flow velocity (V_{auto}) and derived QFR_{auto} using the same reconstructed geometry and QFR algorithm as the main publication. The angiographic image runs and their analysis files were taken from the core laboratory analysis of the FAVOR II China study [8]. Subsequently, QFR_{auto} was assessed in all interrogated vessels with paired QFR_{count} and FFR values. Finally, QFR_{auto} was compared with QFR_{count} and with fixed-flow based QFR (QFR_{fixed}) [6] that did not incorporate patient-specific flow in the QFR computation, using FFR as the reference standard. The study procedure was approved by the institutional review board. All patients provided written informed consent.

The velocity computation algorithm had three major steps: (1) segmentation of coronary vascular structures; (2) extraction of coronary centerlines; and (3) calculation of flow velocity from the extracted centerlines.

Delineation of coronary vascular structures

Segmentation of coronary lumen was performed with the following steps: (1) Image preprocessing techniques [11, 12] were applied to reduce the image noise and increase the local image contrast. (2) Subsequently, a vascular detection algorithm based on Gabor filtering [13] was applied to identify the tube-shaped vascular structures. (3) Finally, the connected region with maximum size was extracted as the targeted vascular structures.

Centerline detection

From the delineated targeted vascular structures, the centerlines of all vascular branches were extracted to obtain lengths of the target vessel within different frames from coronary angiographic image runs that included the entire filling process of contrast dye in coronary arteries. The centerlines of the whole coronary tree were tracked with the following steps: (1) An initialization point [14] was determined as the point in the vascular area with maximum distance to the vascular boundary. (2) Subsequently, the fast marching method [15–17] was applied to derive the evolution time of each pixel in the vascular area, beginning from the initialization point. (3) Finally, the centerlines of all vascular segments were detected from the automatically computed point along the gradient descent of the evolution time. The proximal point was set as the start point of the centerline, while the distal point was set as the end point of the centerline for each segment.

Velocity computation

After extracting the centerlines of the entire vascular structures, the centerline of the interrogated vessel was identified at each image frame using prior knowledge of the interrogated vessel in the angiographic reconstruction [6]. Subsequently, the period with increase in centerline length that corresponded to the period of contrast dye injection was identified. The centerline length and the corresponding frame number were then paired. From the paired points a linear fitting line was automatically generated with the least squared distance between the fitting line and the paired points. The slope of the fitting line was used to compute flow velocity based on the following formula:

$$\text{Velocity} = w \times k \times c \times f$$

where k was the fitting slope, c was the angiographic image calibration factor, f was the angiographic image acquisition frame rate that was stored in the angiographic image DICOM files, and w was the parameter to compensate the effect of vessel foreshortening [18]. The correlation coefficient of the linear fitting line was used as the stability parameter to quantify the contrast flow stability. For the two velocities calculated from two angiographic image runs, the one with better stability was chosen to be the final velocity, denoted as V_{auto}. Figures 1 and 2 showed two examples of the segmentation, centerline detection, and velocity computation procedures of LAD and RCA, as well as the selection of final V_{auto} according to flow stability parameter.

Computation of QFR_{auto}

From the reconstructed geometry that was exported from the core laboratories analysis in the FAVOR II China study [8] and the new computed flow velocity V_{auto}, QFR_{auto} was computed based on the same fluid dynamic algorithms that were used in the commercialized QFR measurement system (AngioPlus 1.0, Pulse medical imaging technology, Shanghai) [8].

Statistical analysis

Continuous variables were described as mean ± standard deviation if not otherwise specified. Correlation was determined by Pearson or Spearman correlation as appropriate. Pair-wise comparisons were performed by Student *t* test or by Mann–Whitney *U* test as appropriate. The difference in velocity computations and in QFR computations by different methods were evaluated by Bland–Altman plots and intraclass correlation coefficients for the absolute agreement. The performance of QFR_{auto} for diagnosis of hemodynamically-significant stenosis was evaluated by overall accuracy, sensitivity, specificity, positive predictive value (PPV), negative predictive value (NPV), positive likelihood ratio (+LR), and negative likelihood ratio (−LR), with FFR ≤ 0.80 as the reference standard to define functional significance, and the 95% confidence intervals were added as appropriate. Comparisons of receiver operator characteristic (ROC) curves were performed by the DeLong method. Analysis of correlation and pair-wise comparisons were performed with IBM SPSS version 22.0 (SPSS Inc., Chicago, Illinois). Other statistical analyses were performed with MedCalc version 14.12 (MedCalc Software, Mariakerke, Belgium). A two-sided p value of < 0.05 defined statistical significance.

Result

All angiographic image data and corresponding values of QFR_{count}, QFR_{fixed} and FFR in 328 interrogated vessels from 304 patients were obtained from the core laboratory analysis in the FAVOR II China study [8]. Using the same angiographic image runs, V_{auto} and QFR_{auto} were automatically calculated. In three interrogated vessels from three patients, V_{auto} and QFR_{auto} could not be calculated due to unacceptable stability in contrast dye filling. Thus, a total of 325 vessels from 301 patients were included for statistical analysis.

Correlation and agreement analyses

Mean V_{auto} was 0.17 ± 0.06 m/s. There was a weak to moderate correlation ($r = 0.37$, $p < 0.001$) and agreement (mean difference: −0.02 ± 0.07 m/s, $p < 0.001$) between V_{auto} and V_{count} (Fig. 3). Poor intraclass correlation was observed (0.35, 95% CI 0.25–0.45). Nevertheless, good correlation ($r = 0.96$, $p < 0.001$) and agreement (mean difference: −0.01 ± 0.04, $p < 0.001$) between QFR_{auto} and QFR_{count} was observed (Fig. 4), and excellent intraclass correlation was observed (0.95, 95% CI 0.93–0.96). There was also good correlation ($r = 0.83$, $p < 0.001$) and agreement (mean difference: 0.01 ± 0.06, $p = 0.016$) between QFR_{auto} and wire-based FFR (Fig. 5), and good intraclass correlation was observed (0.84, 95% CI 0.81–0.87).

Diagnostic performance of the QFR_{auto} using FFR as the reference standard

Using the cutoff value of FFR ≤ 0.80, the area under the receiver-operating characteristic curve (AUC) of QFR_{auto} was 0.97 (95% CI 0.94–0.98). The overall diagnostic accuracy of $QFR_{auto} \leq 0.80$ in predicting FFR ≤ 0.80 was 93.2% (95% CI 90.5–96.0%), with sensitivity and specificity of 92.4% (95% CI 86.0–96.5%) and 93.7% (95% CI 89.5–96.6%), respectively. PPV, NPV, (+)LR and (−)LR of QFR_{auto} were 89.3% (95% CI 82.5–94.2%), 95.6% (95%

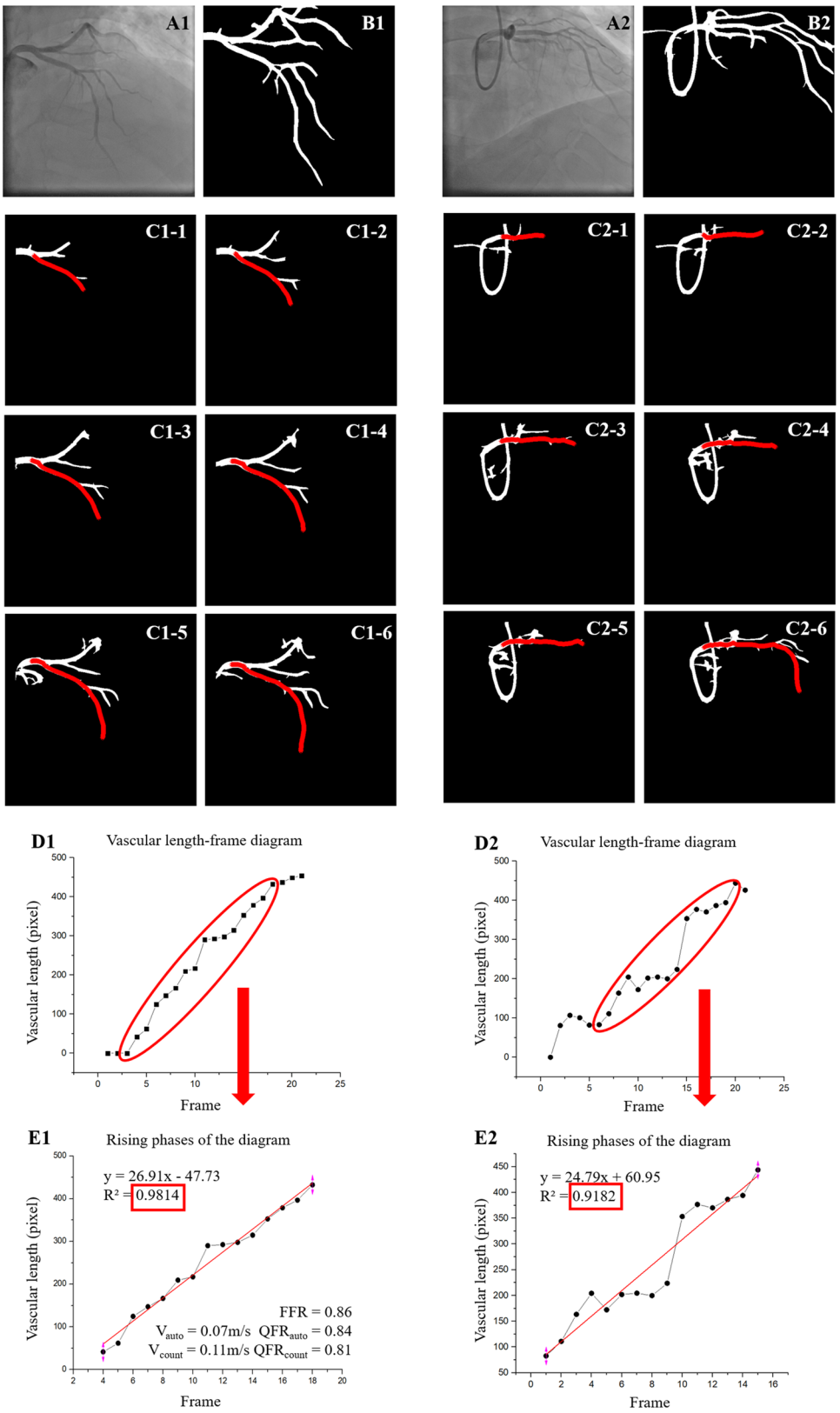

Fig. 1 Demonstration of velocity computation from angiographic image runs for a LAD. A1 and A2 show two angiographic views for QFR computation. B1 and B2 are the results of segmentation after contrast filling. C1 (1–6) and C2 (1–6) show the results of LAD centerline detection during the contrast dye filling process. D1 and D2 show the changes in LAD centerline length with respect to the image frames. The phase with increasing length corresponds to the period of contrast dye injection. E1 and E2 show the linear fitting curves for the two angiographic image runs. The left projection has higher fitting coefficient, suggesting better stability in contrast flow filling. Thus, the left projection was automatically chosen as the projection to compute QFR_{auto}. *LAD* left descending artery, V_{auto} automatically calculated flow velocity, V_{count} frame count-based flow velocity, *QFR* quantitative flow ratio, QFR_{auto} QFR computed by V_{auto}, QFR_{count} QFR computed by V_{count}

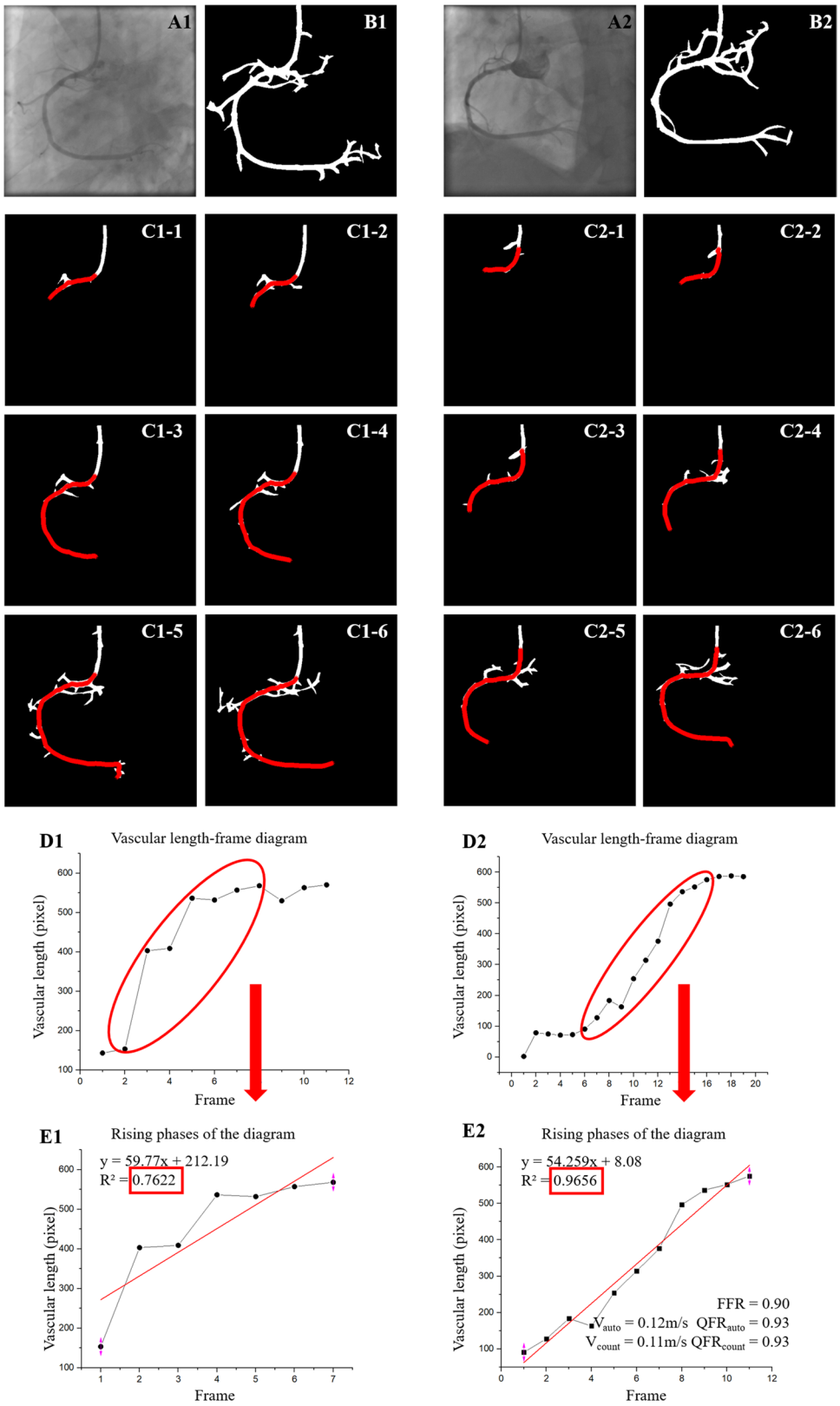

Fig. 2 Demonstration of velocity computation from angiographic image runs for a RCA. A1 and A2 show two angiographic views for QFR computation. B1 and B2 are the results of segmentation after contrast filling. C1 (1–6) and C2 (1–6) show the results of RCA centerline detection during the contrast dye filling process. D1 and D2 show the changes in RCA centerline length with respect to the image frames. The phase with increasing length corresponds to the period of contrast dye injection. E1 and E2 show the linear fitting curves for the two angiographic image runs. The right projection has higher fitting coefficient, suggesting better stability in contrast flow filling. Thus, the right projection was automatically chosen as the projection to compute QFR_{auto}. Abbreviations as in Fig. 1

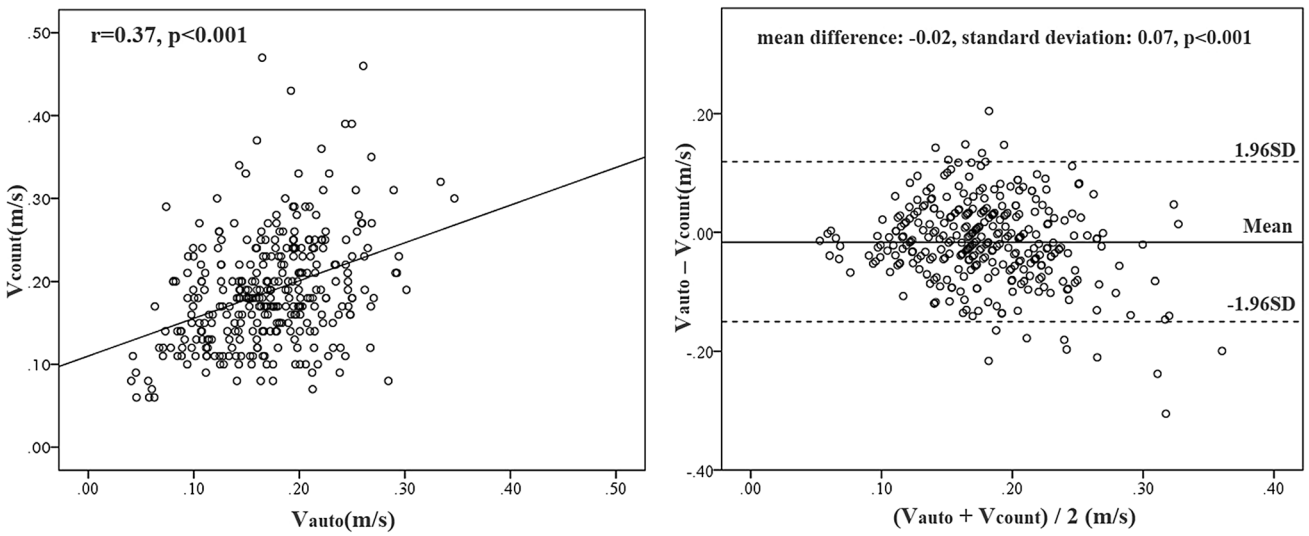

Fig. 3 Correlation and agreement between automatic velocity V_{auto} and frame-counting velocity V_{count}. Weak to moderate correlation and agreement was observed between V_{count} and V_{auto}. Abbreviations as in Fig. 1

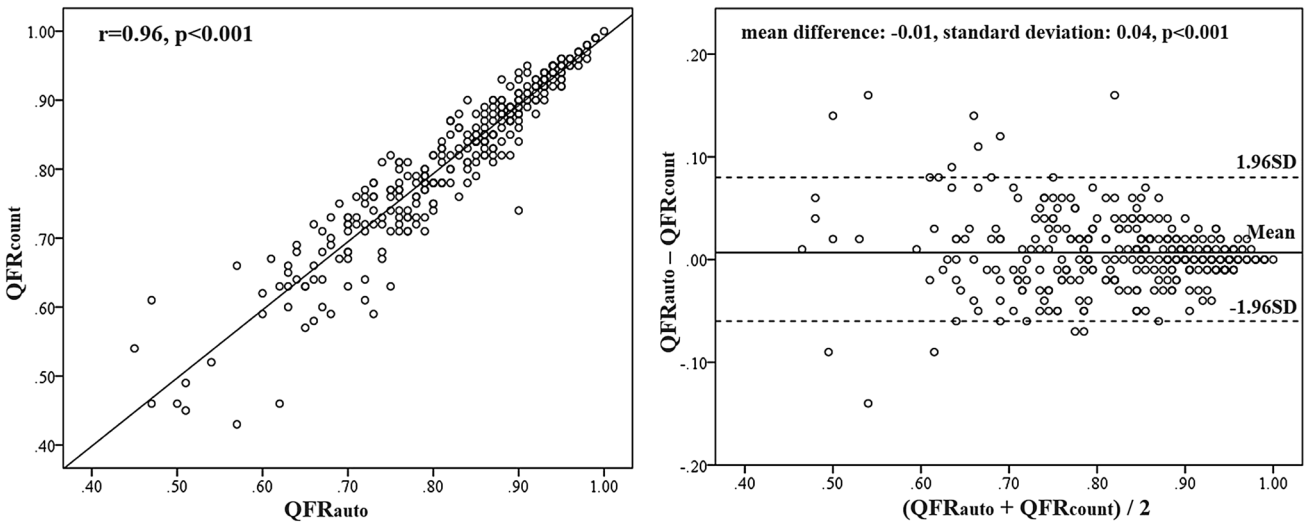

Fig. 4 Correlation and agreement between QFR_{auto} and QFR_{count}. Good correlation and agreement was observed between QFR_{count} and QFR_{auto}. Abbreviations as in Fig. 1

CI 91.8–98.0%), 14.7 (95% CI 8.7–25.0) and 0.1 (95% CI 0.0–0.2), respectively.

Pairwise comparisons between the ROC curves of QFR_{count}, QFR_{fixed} and QFR_{auto} in diagnosis of functionally significant stenosis are shown in Fig. 6. Using FFR as the reference standard, QFR_{auto} had similar diagnostic performance as QFR_{count} (difference in AUC: 0.00; 95% CI −0.01 to 0.01; p = 0.529), while the diagnostic performance of QFR_{auto} was better than that of QFR_{fixed} (difference in AUC: 0.02; 95% CI 0.01–0.03; p = 0.005).

Discussion

This is the first study to validate a novel approach for automatic computation of contrast flow velocity (V_{auto}) to derive QFR from angiographic images, with FFR as the reference standard. The main findings were: (I) Automatic computation of contrast velocity is feasible in an all-comer population; (II) V_{auto} had a modest correlation and agreement with frame count derived contrast flow velocity

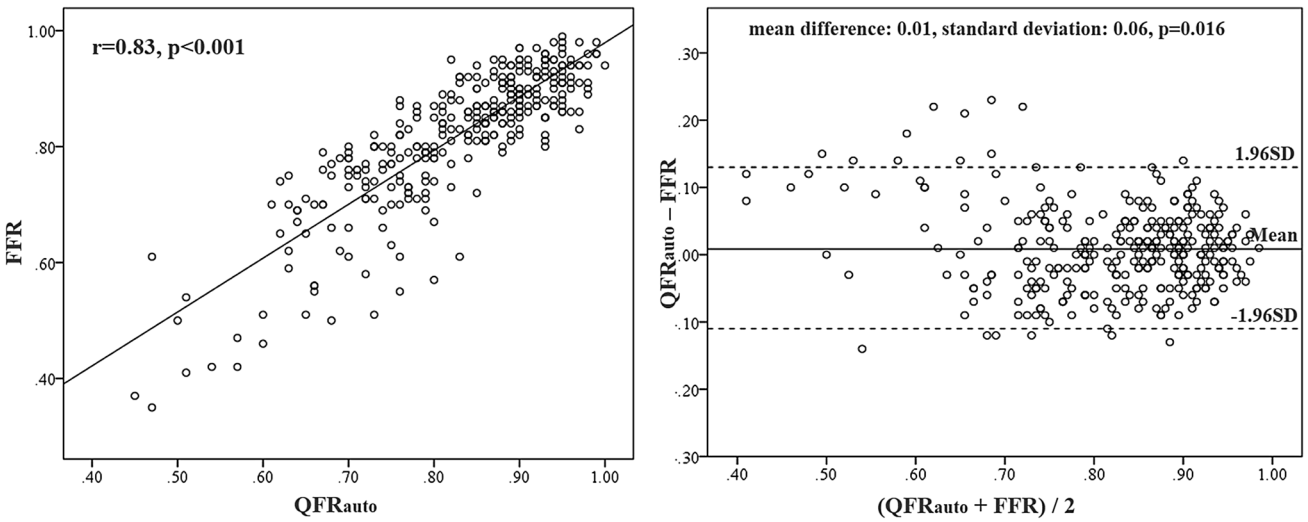

Fig. 5 Correlation and agreement between FFR and QFR_{auto}. Good correlation and agreement was observed between QFR_{auto} and pressure wire-based FFR. *FFR* fractional flow reserve, other abbreviations as in Fig. 1

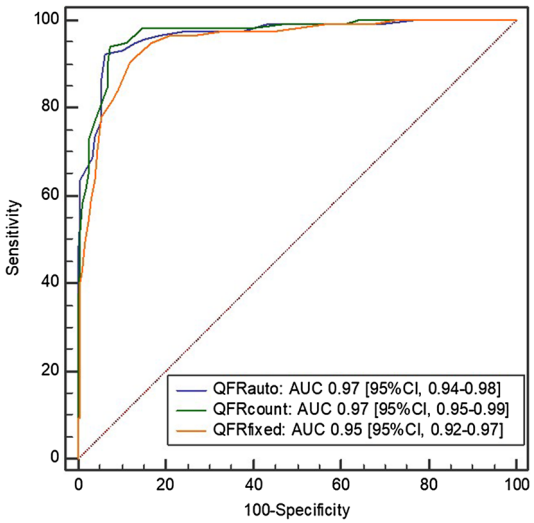

Fig. 6 Comparison of receiver operating curves for the diagnostic performance. The AUC of QFR_{auto} was significantly higher than QFR_{fixed} and had no significant difference with QFR_{count}. *AUC* areas under the receiver-operator characteristics curve, QFR_{fixed} QFR computed by using a fixed flow velocity. Other abbreviations as in Fig. 1

(V_{count}); (III) QFR computed with V_{auto} had a similar diagnostic accuracy compared to QFR computed with V_{count}.

Accurate diagnosis of flow-limiting coronary stenosis is of foremost importance to guide percutaneous coronary interventions in patients with coronary artery disease. Novel functional assessment tools such as FFR have recently challenged the frequently used degree of luminal narrowing by standard coronary angiography [1–5, 19, 20]. However, the wide application of FFR is still limited due to use of pressure wires and hyperemia-inducing medications [21]. QFR, a novel method for fast FFR computation, recently showed good diagnostic performance in both on-line and off-line settings [6–10]. The present QFR application requires substantial user-interaction to derive the 3D vessel reconstruction and to perform the TIMI frame counting. By replacing semi-automatic frame count analysis, our proposed method for automatic velocity computation was feasible (V_{auto} acquired in 99% of dataset) and thus QFR-related user-interaction was decreased.

The weak to moderate correlation ($r=0.37$, $p<0.001$) and agreement (mean difference: -0.02 ± 0.07, $p<0.001$) between V_{count} and V_{auto} was expected since the frame count-based FFR computation requires qualified analysts to accurately determine the start and end frames for contrast dye in the vessel of interest. Furthermore, the analyst is required to manually select an angiographic projection with sufficient image quality which may induce errors related to abnormal dye-flowing during cardiac systole or contrast backflow. On the contrary, our proposed automated method includes a contrast flow stability parameter to automatically quantify the stability of contrast flow passing through the vessel of interest. This allows for more objective identification of angiographic images with steady perfusion of contrast dye. However, in the computation of V_{auto} we used the same value to compensate the foreshortening effect in different cardiac phases. This might reduce the accuracy of V_{auto} due to possible change in vascular shape during heart contraction. These key differences may explain the weak to moderate correlation of frame count derived contrast flow and our proposed automated approach. However, the agreement of QFR_{auto} and QFR_{count} ($r=0.96$, $p<0.001$; difference: -0.01 ± 0.04, $p<0.001$) was excellent. This could be explained by computational characteristics of QFR. Compared with semi-automatic frame count-based flow velocity, V_{auto}

systematically underestimated flow velocity by 0.02 m/s with a standard deviation of 0.07 m/s. This standard deviation value was about 20% of the mean hyperemic flow velocity (0.35 m/s) [6]. For the present study population with predominately intermediate stenosis with minimal flow disturbance, the pressure drop is mainly caused by the viscous friction in the stenotic segment which has a linear correlation with the flow rate [22]. Assuming an intermediate stenosis with an FFR of 0.80, an underestimation of flow by 20% will result in a computational FFR of 0.84 (about 20% less pressure drop). While in clinical routine of FFR measurement, a pullback with pressure drift of less than 0.05 is often acceptable. Therefore, the impact on computational FFR by the precision in the estimation of V_{auto} appears to be clinically acceptable.

QFR_{fixed} allows for QFR computation with a fixed hyperemic flow velocity of 0.35 m/s and thus user-interaction and observer variations are thus avoided. In the FAVOR II China [8], both QFR_{fixed} ($r = 0.82$, $p < 0.001$; difference: 0.00 ± 0.07, $p < 0.001$) and QFR_{count} ($r = 0.86$, $p < 0.001$; difference: 0.00 ± 0.06, $p < 0.001$) showed good correlation and agreement with FFR. Interestingly, our findings demonstrate that QFR_{auto} has a slightly better diagnostic performance than QFR_{fixed} ($p = 0.005$) with FFR as the reference standard. These results indicate that QFR_{auto} preserves the advantage of patient-specific velocity that appears to be significant for some patient groups such as patients with microcirculatory dysfunction [23]. The clinical importance of these small differences is unknown and should be assessed in future studies.

Study limitations

Our computation approach requires a steady contrast dye flow. Insufficient contrast injection or unable to align the diagnostic guiding catheter co-axially to the interrogated vessel might affect vessel delineation and contrast filling, deteriorating the reliability of automatic flow velocity assessment. Manual injection of contrast dye was applied to the majority of the current study population. It is unclear that whether use of automatic contrast injection would improve the computational QFR or not. The FAVOR II China study presented the best diagnostic performance estimates for QFR to date, most likely mediated by optimized angiographic quality based on QFR-specific standard procedures. Hence, for angiographic images of suboptimal quality, our approach might have limitations.

Conclusion

Automatic contrast flow velocity computation from coronary angiographic images is a novel and feasible method to improve the QFR computational process. QFR computation based on the proposed automated approach may reduce QFR-related inter- and intra-observer variation without compromising the diagnostic accuracy.

Funding This study was supported by the National Key Research and Development Program of China (Grant No. 2016YFC0100500), the Natural Science Foundation of China (Grant No. 81871460 and 31500797), Shanghai ShenKang Hospital Development Center (16CR3034A), and Shanghai Jiao Tong University (Grant No. YG2015ZD04 and YG2016ZD09).

Compliance with ethical standards

Conflict of interest None of the Authors have declared a conflict of interest in relation to this study, with the exception that S Tu received research support from Medis medical imaging and Pulse medical imaging. Other authors report no conflicts of interest regarding this manuscript.

References

1. De Bruyne B, Pijls NHJ, Kalesan B et al (2012) Fractional flow reserve–guided PCI versus medical therapy in stable coronary disease. N Engl J Med 367(11):991–1001
2. Tonino PAL, De Bruyne B, Pijls NHJ et al (2009) Fractional flow reserve versus angiography for guiding percutaneous coronary intervention. N Engl J Med 360(3):213–224
3. Johnson NP, Tóth GG, Lai D et al (2014) Prognostic value of fractional flow reserve: linking physiologic severity to clinical outcomes. J Am Coll Cardiol 64(16):1641–1654
4. Berry C, Corcoran D, Hennigan B et al (2015) Fractional flow reserve-guided management in stable coronary disease and acute myocardial infarction: recent developments. Eur Heart J 36(45):3155–3164
5. Fearon WF (2014) Percutaneous coronary intervention should be guided by fractional flow reserve measurement response to Fearon. Circulation 129(18):1860–1870
6. Tu S, Westra J, Yang J et al (2016) Diagnostic accuracy of fast computational approaches to derive fractional flow reserve from diagnostic coronary angiography: the international multicenter FAVOR pilot study. JACC Cardiovasc Interv 9(19):2024–2035
7. Tu S, Barbato E, Köszegi Z et al (2014) Fractional flow reserve calculation from 3-dimensional quantitative coronary angiography and TIMI frame count: a fast computer model to quantify the functional significance of moderately obstructed coronary arteries. JACC Cardiovasc Interv 7(7):768
8. Xu B, Tu S, Qiao S et al (2017) Diagnostic accuracy of angiography-based quantitative flow ratio measurements for online assessment of coronary stenosis. J Am Coll Cardiol 70(25):3077–3087
9. Westra J, Tu S, Winther S et al (2018) Evaluation of coronary artery stenosis by quantitative flow ratio during invasive coronary angiography: the WIFI II study (wire-free functional imaging II). Circ Cardiovasc Imaging 11(3):e007107
10. Westra J, Andersen BK, Campo G et al (2018) Diagnostic performance of in-procedure angiography-derived quantitative flow reserve compared to pressure-derived fractional flow reserve: the FAVOR II Europe-Japan Study. J Am Heart Assoc Cardiovas Cerebrovasc Dis 7(14):e009603
11. Perona P, Malik J (2002) Scale-space and edge detection using anisotropic diffusion. IEEE Trans Pattern Anal Mach Intell 12(7):629–639

12. Jin Y, Fayad LM, Laine AF (2001) Contrast enhancement by multiscale adaptive histogram equalization. In: International symposium on optical science and technology. International society for optics and photonics
13. Prasad VSN, Domke J (2005) Gabor filter visualization. J Atmos Sci 13
14. Osher S, Sethian JA (1988) Fronts propagating with curvature-dependent speed: algorithms based on Hamilton-Jacobi formulations. J Comput Phys 79:12–49
15. Hassouna MS, Farag AA (2007) Multistencils fast marching methods: a highly accurate solution to the Eikonal equation on Cartesian domains. IEEE Trans Pattern Anal Mach Intell 29(9):1563–1574
16. Godunov SK (1959) A finite difference method for the numerical computation of discontinuous solutions of the equations of fluid dynamics. Matematicheskii Sbornik 47:357–393
17. Van Uitert R, Bitter I (2007) Subvoxel precise skeletons of volumetric data based on fast marching methods. Med Phys 34(2):627
18. Tu S, Hao P, Koning G et al (2011) In vivo assessment of optimal viewing angles from X-ray coronary angiography. Eurointervention 7(1):112
19. Toth G, Hamilos M, Pyxaras S et al (2014) Evolving concepts of angiogram: fractional flow reserve discordances in 4000 coronary stenoses. Eur Heart J 35(40):2831–2838
20. Tu S, Echavarria-Pinto M, Birgelen CV et al (2015) Fractional flow reserve and coronary bifurcation anatomy: a novel quantitative model to assess and report the stenosis severity of bifurcation lesions. JACC Cardiovasc Interv 8(4):564–574
21. Götberg M, Fröbert O (2017) Instantaneous wave-free ratio versus fractional flow reserve. N Engl J Med 377(16):1813–1823
22. Gould KL (1978) Pressure-flow characteristics of coronary stenoses in unsedated dogs at rest and during coronary vasodilation. Circ Res 43(2):242–253
23. Mejía-Rentería H, Lee JM, Lauri F et al (2018) Influence of microcirculatory dysfunction on angiography-based functional assessment of coronary stenoses. JACC Cardiovasc Interv 11(8):741–753